RESEARCH ARTICLE

Paul J. Stapley · Thierry Pozzo · Guy Cheron
Alexander Grishin

Does the coordination between posture and movement during human whole-body reaching ensure center of mass stabilization?

Abstract The whole-body center of mass (CoM) has been classically regarded as the stabilized reference value for human voluntary movements executed upon a fixed base of support. Axial synergies (opposing displacements of head and trunk with hip segments) are believed to minimize antero-posterior (A/P) CoM displacements during forward trunk movements. It is also widely accepted that anticipatory postural adjustments (APAs) create forces of inertia that counteract disturbances arising from the moving segment(s). In the present study, we investigated CoM stabilization by axial synergies and APAs during a whole-body reaching task. Subjects reached towards an object placed on the ground in front of them in their sagittal plane using a strategy of coordinated trunk, knee, and hip flexion. The reaching task imposed constraints on arm-trajectory formation and equilibrium maintenance. To manipulate equilibrium constraints, differing conditions of distance and speed were imposed. The comparison of distance conditions suggested that axial synergies were not entirely devoted to CoM stabilization: backward A/P hip displacements reduced as head and trunk forward A/P displacements increased. Analysis of upper- and lower-body centers of mass in relation to the CoM also showed no strict minimization of A/P CoM displacements. Mechanical analysis of the effects of APAs revealed that, rather than acting to stabilize the CoM, APAs created necessary conditions for forward CoM displacement within the base of support in each condition. The results have implications for the CoM as the primary stabilized reference for posture and movement coordination during whole-body reaching and for the central control of posture and voluntary movement.

Key words Coordination · Posture · Movement · Anticipatory postural adjustments · Axial synergy · Human

P.J. Stapley (✉) · T. Pozzo
Groupe d'Analyse du Mouvement (GAM),
UFR STAPS BP 27877, Université de Bourgogne,
F-21078 Dijon Cedex, France,
Tel.: 00 33-380-39 67 48, Fax: 00 33-380-39 67 02

G. Cheron
Laboratory of Biomechanics, Université Libre de Bruxelles,
Avenue P. Heger, CP 168, B-1050 Brussels, Belgium

A. Grishin
Institute for Problems of Information Transmission (IPIT),
Russian Academy of Sciences, B. Karenty per. 19,
GSP-4 Moscow, Russia

Introduction

A great deal of evidence surrounds differing interpretations of stabilized reference values for posture and voluntary movement coordination. The feed-forward stabilization of the head for the optimization of gaze has been shown to be an important element of the postural-control system during locomotor (Pozzo et al. 1990) and other complex equilibrium tasks (Pozzo et al. 1995). The position of a segment in space may also be stabilized, but is dependent upon task constraints (Marsden et al. 1981; Droulez and Berthoz 1986). Trunk stabilization or the optimization of trunk position with respect to the vertical has been shown to ensure that the trunk becomes an egocentric reference value for posture and movement coordination in humans (Mergner et al. 1991; Mouchnino et al. 1993). However, during conditions of static and dynamic equilibrium, the stabilized reference has been recognized as being the maintenance of the projection of the whole-body center of mass (CoM) within the base of support (BoS). This idea of the CoM as the stabilized reference value in human bipeds is highly recurrent throughout the literature, having been adopted for explaining findings of the study of posture and movement coordination with changing BoS configuration (Mouchnino et al. 1992; Nardone and Schiepatti 1988), moving segment(s) (Bouisset and Zattara 1981; Crenna et al. 1987), or environmental conditions (Mouchnino et al. 1996; Massion et al. 1997).

Two control mechanisms have been described to facilitate the link between posture and movement coordi-

nation and to minimize perturbations to the body CoM. First, postural or "*axial*" synergies, described as coordinated, opposing displacements of upper and lower body segments (first noted by Babinski 1899), have been shown to minimize CoM displacements during forward (and backward) trunk bending (Crenna et al. 1987; Oddsson 1988; Pedotti et al. 1989; Alexandrov et al. 1998). Indeed, Ramos and Stark (1990), using modeling techniques, showed that forward trunk-bending movements without backward postural adjustments at the hips led to CoM antero-posterior (A/P) displacements of up to 12 cm. From a mechanical perspective, Eng et al. (1992) demonstrated that the interaction of reactive joint torques and the offsetting of individual mass centers of focal and postural segments ensured whole-body CoM stabilization during bilateral arm movements. Second, feed-forward commands activating leg muscles involved in postural control, so-called anticipatory postural adjustments (APAs), have been interpreted as creating forces of inertia that counteract external or internal forces arising from the mobile segment(s), thus minimizing CoM perturbations (Bouisset and Zattara 1981, 1987). Therefore, it is commonly accepted that these two control strategies can stabilize the position of the CoM and prevent disequilibrium during voluntary movement execution.

The present study investigated displacements of the CoM, sagittal plane body kinematics, APAs, and whole-body dynamics accompanying forward whole-body reaching movements with the aim of answering the following question: is the CoM the stabilized reference value during posture and movement coordination in this particular task? A previous study from our group (Pozzo et al. 1998) has shown that whole-body reaching movements demonstrate opposing displacements of the head and trunk with the hips, similar to those described as efficiently minimizing CoM displacements during forward trunk bending (Crenna et al. 1987). In this study, we intended to examine if such "axial" strategies for CoM stabilization can be generalized to other forward-oriented movements (in this case, whole-body reaching) involving significant displacements of the trunk and across changing equilibrium conditions. A preliminary study (Stapley et al. 1998) also showed that, contrary to classical ideas, anticipatory muscular activity of the lower limbs create the necessary dynamic conditions for forward CoM displacement during whole-body reaching to objects placed at a distance of 30% of each subject's height. It may be argued that APAs perform such an initiatory role because large-amplitude reaching movements necessitate a forward displacement of the CoM. In the present study, we compared smaller-amplitude reaching movements (where a stabilization of the CoM could more easily be attained) with larger-amplitude movements in order to be able to generalize the role of APAs as initiating, as opposed to stabilizing actions during this task.

If segmental strategies (axial synergies) do not correctly stabilize the CoM and the role of APAs in displacing the CoM within the BoS can be generalized across

movement amplitudes, new speculations about the central control of movement and posture may be made. One theory behind posture and movement control is of separate descending pathways, one responsible for movement control, the other for the maintenance of equilibrium (Massion 1992). If we can show that, during whole-body reaching, the CoM is displaced in the direction of the movement by anticipatory muscular activity, it may be proposed that the CNS programs posture and movement together (a common controller) to ensure the smooth transition from one posture to another. Also, the idea that the CoM is displaced by APAs has, until now, only been considered for the initiation of locomotion (Brenière et al. 1987) where the BoS constantly changes. In one particular study, Lee et al. (1990) hypothesized that subjects obtained additional arm-pulling force by making a backward body rotation through anticipatory ankle activity. Generally however, the idea that APAs initiate significant CoM displacements within a fixed BoS has not been proposed. Moreover, the whole-body reaching model represents an original approach to the study of posture and movement coordination, which has traditionally looked at the perturbing effects of non-goal-directed voluntary movements imposed upon essentially static postural configurations.

Materials and methods

Subjects

Six healthy subjects (four males and two females, aged between 18 and 29 years, mean height 1.70 ± 0.05 m, weight 71.4 ± 8.7 kg, and foot size 0.245 ± 0.059 m), with no previous history of neuromuscular disease, participated in this study. Written consent was obtained following guidelines of the University of Burgundy.

Protocol

Throughout all testing sessions, subjects were initially asked to adopt an erect standing posture with the arms in front of the body, hands crossed, the left palm covering the right hand, both comfortably placed against the body at the level of the navel. Subjects were asked to grasp a wooden dowel (0.40 m long, 0.07 m in diameter, and 1.8 kg in weight), mounted on two, 0.15 m semi-circular supports and placed at ground level in front of them in their sagittal plane. Following object grasp, subjects lifted the object to shoulder height, where they retained a stationary upright posture. No formal indications were given as to the strategy required to reach, grasp, and lift the object; subjects were asked, however, not to support their body weight on the dowel. To control for this, all trials where the center of foot pressure (CoP) clearly left the base of support (BoS) were eliminated from the analysis (approximately 10% of all trials executed, indicating either a forward fall or subjects supporting themselves on the dowel). All subjects adopted a strategy of coordinated trunk, knee, and hip flexion to reach the object, grasping it using an open-fisted cylindrical grasp. Each subject began by executing one block of four reach-to-lift movements at normally paced speed (N) towards a first object distance (D1=5% of body height), measured from the distal end of subjects great toe. This was followed by another block of four trials, still at D1, as fast as possible (F). This order was repeated for a further two blocks of four trials made to a second object distance (D2=30% of body height). Thus, during testing sessions, each subject conducted a total of four blocks (D1 N, D1 F, D2 N and D2 F)

of four trials (totaling 16 reach-to-lift movements), each block being separated by 3 min rest periods. Data analysis was based upon a total of 86 trials (distance and speed conditions pooled). Acquisitions began at least 1 s before a tone signal, upon which subjects were asked to reach. During a practice period of approximately 5 min, subjects executed reach-to-lift movements twice at each distance and speed (eight trials).

Apparatus

Two infra-red-emitting cameras placed 3 m from the subjects' sagittal axis, one on top of the other and 1 m and 2 m from the ground, recorded movements of 11 retro-reflective markers (15 mm in diameter) placed at different anatomical sites using an optoelectronic measuring device ELITE (BTS Milan Italy) at a sampling frequency of 100 Hz. Markers were placed on each subject's left side at the following sites: the head (external canthus of the eye and the auditory meatus of the ear), the trunk (the lumbosacral L5-S1 vertebra), the lower limb (the greater trochanter, the knee interstitial joint space, the ankle external malleolus, and the foot fifth metatarsophalangeal), and the upper limb (acromial process of the shoulder, the lateral condyle of the elbow, the styloid process of the wrist and the fifth metacarpophalangeal).

A/P (Fx), vertical (Fz), and mediolateral (Fy) ground reaction forces and the position of the CoP were recorded using an AMTI (Watertown, USA) force platform at a sampling rate of 500 Hz. Electromyographic (EMG) signals were obtained using pairs of bipolar silver-chloride surface electrodes from the following four pairs of antagonistic muscles: soleus (SOL), tibialis anterior (TA), biceps femoris (BF), vastus lateralis (VL), erector spinae (ES), rectus abdominis (RA), splenus (SP), and sterno-cledio mastoideus (SCM). Electrodes were attached longitudinally over the bulkiest part of each muscle belly with a center-to-center electrode distance of 25 mm, using standard skin-preparation procedures (Basmajian 1978). For the SOL muscle, electrodes were placed medially at its protrusion below the gastrocnemius medialis. Signals were sampled at 500 Hz, band-pass filtered between 6–200 Hz, rectified, and normalized as a percentage of maximal activation values. For each trial, EMG burst onsets were identified initially by visual inspection and quantitatively from the moment when activity exceeded mean tonic levels (measured over 200 ms between –500 and –300 ms before mechanical trace onset) plus two standard deviations (SDs) of the mean. Bursts were considered only if they exceeded this threshold for a period of time longer than 30 ms. Inhibitions or silent periods were also identified by initial visual inspection and from when activity dropped below mean tonic levels minus one SD for a time period greater than 30 ms. The analysis of EMG activity was based upon each muscles activation or inhibition latencies relative to focal movement onset (explained below). As part of the analysis of APAs, latencies to peak amplitudes of the TA muscle were also recorded.

Data analysis

The movement analysis system recorded and reconstructed successive images (every 10 ms) in three dimensions. Kinematic variables were low-pass filtered (digital second-order Butterworth filter, 5 Hz cut-off frequency) and position and velocity parameters were calculated in the A/P (X) and vertical (Z) axes. Data analysis was made only with respect to the anticipation and execution of the reaching phase (to object grasp). Intentional (focal) movement onsets (t0) and ends were established using wrist curvilinear velocity profiles. From their bell-shaped characteristics, t0 was defined in the first instance from the initial 10 ms period where wrist curvilinear velocities showed sustained deflections above zero. Verifications were made by considering onsets (and ends) only if they exceeded a threshold of 5% of maximum curvilinear velocity during the reaching phase (similar to methods described in Sergio and Ostry 1994). Maximal excursions of linear A/P segmental displacements (at the head, shoulder, hip, and knee) and the various

center of mass displacements (see below) were calculated in the elapsed time between onsets and ends of the focal reaching movement.

Sagittal whole-body CoM positions were calculated using a seven-segment, rigid mathematical model consisting of the following appendicular and axial body segments: head-neck, upper trunk, abdomen-pelvis, thigh, shank, upper arm, and forearm. Foot position was assumed to be bilaterally symmetrical. Using the model, the position of the CoM of an ith segment with co-ordinates X_i, Z_i was calculated using the following formulae:

$$X_i = X1_i + l_i(X2_i - X1_i) \text{ and } Z_i = Z1_i + l_i(Z2_i - Z1_i)$$

where $X1_i$, $Z1_i$, $X2_i$, $Z2_i$ = coordinates of segment ends and l_i = the ratio between the distance of the proximal marker to the segments CoM and its length. Coordinates in X and Z of the whole-body CoM were thus calculated using the formulae:

$$X = \sum m_i X_i / \sum m_i \quad \text{and} \quad Z = \sum m_i Z_i / \sum m_i,$$

m_i being the mass of the ith segment. Anthropometric parameters including segments masses, moments of gyration, and positions of their individual centers of mass were taken from Plagenhoef et al. (1983). The trunk was divided at the L5-S1 level to optimize the determination of the whole-body CoM (see Kingma et al. 1995). Separate CoM calculations were made to evaluate the effectiveness of upper- and lower-body segments in stabilizing the A/P position of the whole-body CoM. An upper-body CoM (CoMu) was calculated using a model incorporating only upper trunk (thorax), head-neck, upper arm, and forearm segments. Also, a lower-body CoM (CoMl) consisted of abdomen-pelvis, thigh, and shank segments. We chose the division between upper- and lower-body segments to be at the L5-S1 level as it was rarely displaced forward during reaching (see Fig. 1). In order to validate the accuracy of the seven-segment model, Pearson coefficients of correlation were calculated between each of the time series of recorded and estimated Fx and Fz ground reaction forces during whole-body reaching. The difference between the CoP and the vertical ground projection of the CoM during quiet stance (300 ms before movement onset) was also calculated. These measures are presented in Table 3. Model-validation techniques and results are discussed in the Appendix.

Whole-body dynamics

To investigate the biomechanical effects of anticipatory muscular activity, the analysis of whole-body dynamics was made adopting methods and variables similar to those used to analyze load-lifting (Toussaint et al. 1995). The magnitude of the resultant ground reaction-force vector (F_R) was determined from Fx, Fz, and Fy values by applying appropriate trigonometric formulae. The angle formed by the tangent of forces Fx and Fz was calculated (every 10 ms) to provide the direction of F_R with respect to the position of the CoM. A measure of the external moment (M_X) was generated by the relation $M_A \times F_R$, with M_A (the moment arm) being the distance between A/P ground projection of the CoM and CoP (the origin of the F_R vector). This external moment (M_X) has been shown to represent a good estimate of whole-body angular momentum (see Toussaint et al. 1995). A/P displacements of the CoM (derived from the model) and CoP (taken from the platform) were expressed as a percentage of the distance between the two foot markers (fifth metatarsophalangeal and external malleolus), giving a measure of relative foot length.

Statistical analysis

Main-effect differences between dependent variables were tested using a 2×2 (two distances: D1 and D2, and two speeds: naturally paced, N, and fast, F) multivariate analysis of variance (MANOVA). Post hoc analysis was conducted using a Neuman-Keuls

test. Kolmogorov-Smirnov tests for normality were used to test for the existence of a normal distribution (each dependent variable). Results showed that the data were normally distributed. Pearson's product moment correlation coefficients were used for any correlations.

Results

General characteristics of whole-body reaching

In all four conditions, whole-body reaching movements demonstrated opposing displacements of body segments similar to those recorded during forward trunk bending (Crenna et al. 1987). Figure 1 illustrates average movements (four trials) for one subject (S6) at D1 and D2 and at both speeds. In general, forward and downward head and shoulder trajectories were accompanied by backward and downward trajectories of abdomen-pelvis and hip markers. The knee showed slightly forward and downward curved trajectories. The wrist displayed initial forward and upward trajectories, followed by large vertical displacements and finishing with marked backwardly oriented curvatures. Average reaching-movement times were: 1140±183.4 (D1 N), 751.7±126.8 (D1 F), 1127.2±176.8 (D2 N) and 801.1±77.1 ms (D2 F). There was a highly significant effect of movement speed ($P<0.001$), but not distance ($P>0.05$) upon the duration of whole-body reaching movements.

Antero-posterior segment displacements

When reaching distant targets, both the knee and shoulder displaced further forward. A surprising finding (shown in Fig. 1) was that, with increasing object distance, there was a reduction in backward hip displacements. This trend was reproduced consistently in all six subjects (see Fig. 2). Statistical analysis revealed main-effect increases in shoulder [$F(1,5)=12.2$, $P<0.001$] and knee [$F(1,5)=32.3$, $P<0.001$] forward displacements as well as significant decreases in backward hip displacements [$F(1,5)=19.8$, $P<0.001$] with increasing object distance. However, no significant changes with distance occurred for head displacements, regardless of movement speed [$F(1,5)=0.22$, $P>0.05$].

Figure 1 also illustrates that forward displacements of both the head and shoulder decreased when subjects executed fast reaching at both distances. Contrary to results of increasing distance, the hip displaced significantly further backwards in F than in N conditions. Compensatory movements with increasing speed of the head, shoulder, and knee (D2) with the hip can be clearly seen in Fig. 1. Modifications to segment displacements with speed were significant for the head [$F(1,5)=11.3$, $P<0.001$], shoulder [$F(1,5)=13.8$, $P<0.001$], and hip [$F(1,5)=30.3$, $P<0.001$], whilst post hoc analysis (a significant interaction effect) revealed significant decreases for the knee only at D2 ($P<0.01$). Figure 2 shows mean A/P displacements (all six sub-
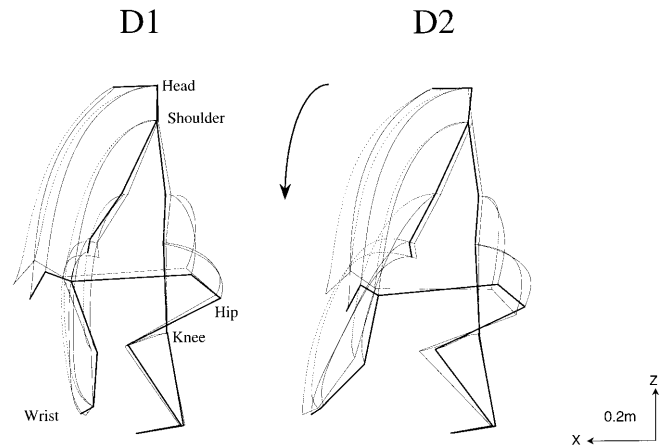

Fig. 1 General characteristics of whole-body reaching movements. Four trials averaged for one subject (S6) in the sagittal plane for movements executed at distances *D1* (5% of height) and *D2* (30% of height), at both naturally paced and fast speeds. Initial and final positions are shown for head, neck, upper trunk, abdomen-pelvis, thigh, shank, foot, upper arm, forearm, and hand segments. *Thin segments* Naturally paced movements, *thick segments* fast movements. Segment trajectories are shown by *dashed* (naturally paced trials) and *full lines* (fast trials). Indicated are the five main anatomical points used in the analysis of axial synergies (head, shoulder, wrist, hip, and knee). *Horizontal and vertical lines* (to the right of the figure) represent the scale (0.2 m) in each axis (X and Z)

jects) for the head, shoulder, wrist, hip, and knee markers in all conditions.

Center-of-mass displacements

Despite the compensatory synergies of the head, shoulder, and hip described above, Fig. 3 shows initial forward A/P, followed by vertical and continuing A/P displacements of the CoM in all subjects and experimental conditions. Forward A/P displacements of the CoM were greatest in the D2 N condition. Actual mean values (all subjects) of A/P CoM amplitudes ranged between 0.032±0.02 m (D1 N) and 0.091±0.021 m (D2 N). This range of values represented 22.1±13.9% and 63.8±16.5%, respectively, of relative BoS length. There were highly significant main effect increases with distance [$F(1,5)=64.9$, $P<0.001$], but decreases with speed [$F(1,5)=16.5$, $P<0.01$] in A/P CoM displacements. Table 1 lists actual mean A/P amplitudes of the CoM, whilst Fig. 4 shows mean CoM displacements in all conditions as a percentage of relative BoS length.

The interaction between upper- and lower-body segments

Figure 3 also shows displacements of the three centers of mass (whole-body CoM, upper-body CoMu, and lower-body CoMl) for all six subjects (means of four trials in each condition). In all conditions, the CoMu displayed

Fig. 2A–E Mean absolute displacements of head, shoulder, wrist, hip, and knee segments for all subjects and experimental conditions. Mean values correspond to *horizontal lines within the rectangles*, the standard error of the mean is the *top* and *bottom of the rectangles*, and the standard deviation is the *upper* and *lower limits of the error bar*. The two stick figures to the right represent initial (*I*) and final (*II*) segment positions, between which total displacements were calculated. Units are shown in m. *D1 N* Distance 1 (5% of height), natural speed; *D1 F* distance 1, fast speed; *D2 N* distance 2 (30% of height), natural speed; *D2 F* distance 2, fast speed
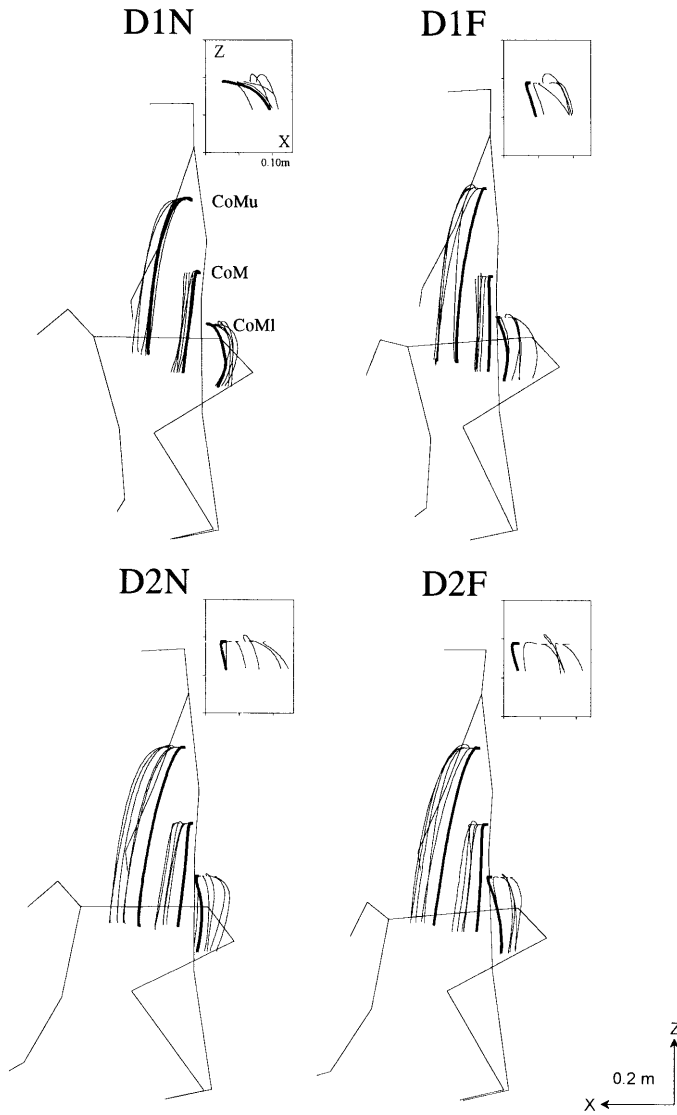
D1N   D1F

D2N   D2F
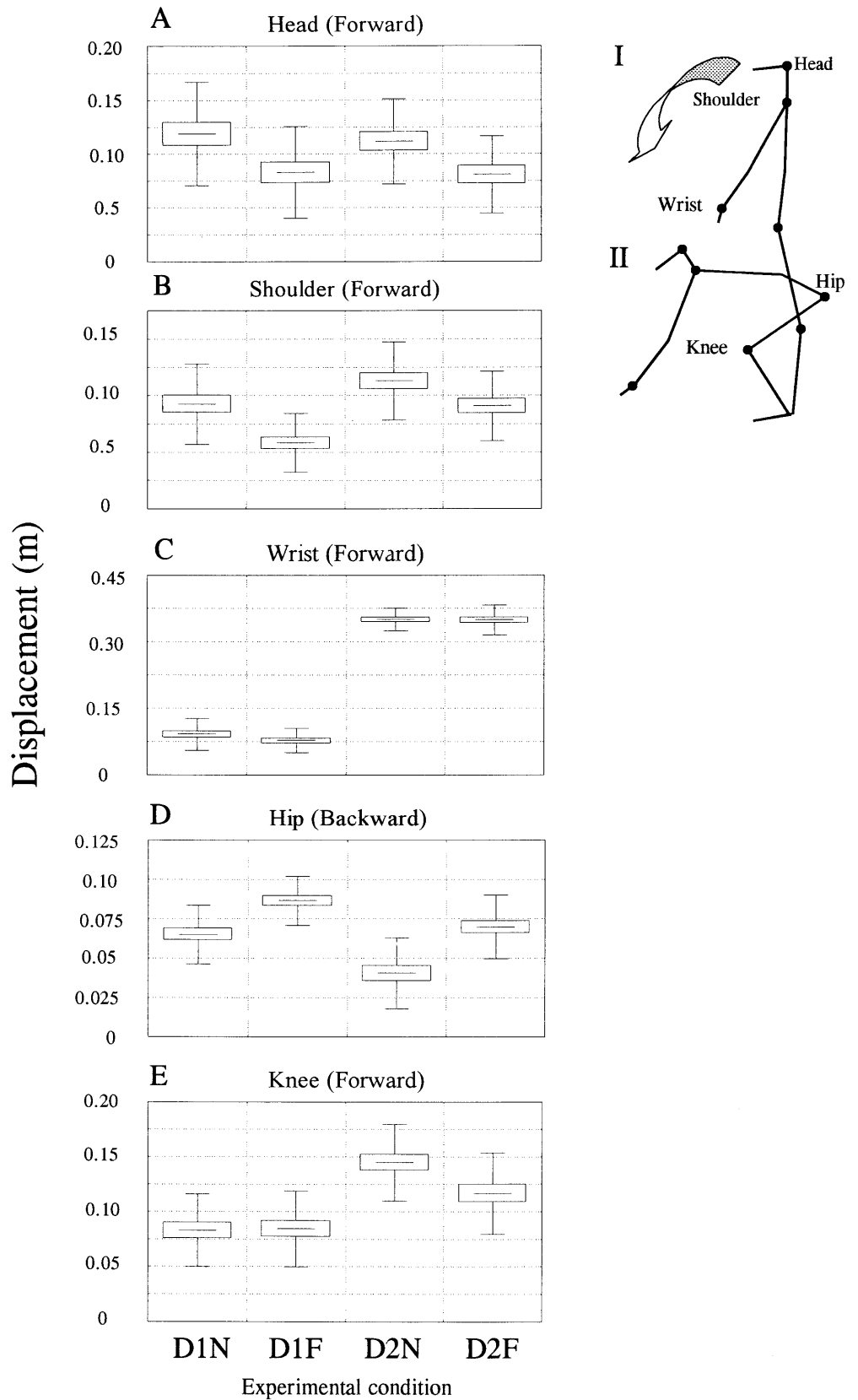
Fig. 3 Mean trajectories (all six subjects) of whole (*CoM*), upper (*CoMu*), and lower body (*CoMl*) centers of mass in each of the four experimental conditions (D1 N, D1 F, D2 N and D2 F, see Fig. 2 for an explanation). Each trajectory represents the mean of four trials for each of the six subjects. *Thicker lines* indicate average CoM trajectories for the subject corresponding to the stick figures, whilst *thinner lines* represent the remaining five subjects. The three CoM trajectories have been normalized in amplitude for each subject so as to correspond to the chosen stick figure. For clarity, CoM and CoMu trajectories have been systematically displaced by 10 mm in the direction of movement (forwards). Likewise, CoMl displacements have also been displaced by 10 mm in the opposite direction to that of the movement (backwards). In each condition, the *inset* (top right) shows initial CoMl trajectories (first 600 ms of naturally paced speed, 300 ms of fast speed conditions)

large displacements initially forwards, then downwards. The CoMl showed initial backward trajectories opposite in polarity to those of the CoMu, but whose displacements reversed approximately midway through reaching movements, such that they followed similar paths to both the CoM and CoMu. Close inspections of initial CoMl
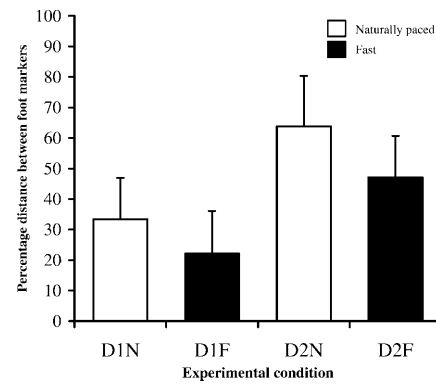

Fig. 4 Mean antero-posterior center-of-mass (CoM) amplitudes (all subjects), expressed as a percentage of relative base of support (BoS) length (the distance between markers placed on the fifth metatarsophalangeal and the external malleolus). *Error bars* indicate plus and minus one standard deviation of the mean. The definition of experimental conditions is given in Fig. 2

trajectories (insets, Fig. 3) revealed that, in three of the four conditions (D1 F in three subjects, D2 N and D2 F, all subjects), there were slight, but noticeable initial forward displacements of the CoMl. Thus, the CoMl could be characterized by up to three phases: a slight initial forward displacement (approximately 62.5% of trials), an intermediate backward displacement, and a final forward displacement in a direction similar to those of both the CoM and CoMu. The analysis of recorded A/P amplitudes of CoMu and CoMl (Table 2) gave highly significant main-effect decreases in backward CoMl displacements [$F(1,5)=18.4$, $P<0.001$] and significant increases in forward displacements of both the CoMu [$F(1,5)=85.4$, $P<0.001$] and CoMl [$F(1,5)=25.2$, $P<0.001$] with distance. CoMu forward displacements were significantly reduced [$F(1,5)=19.2$, $P<0.01$], whereas no changes were recorded in forward [$F(1,5)=2.3$, $P>0.05$] or backward [$F(1,5)=3.6$, $P>0.05$] CoMl displacements with reaching speed.

Electromyographic activity

EMG activity showed a consistent pattern across subjects and conditions. Figure 5A illustrates typical activity (S2, condition D1 F) from the four pairs of antagonistic muscles recorded, and Fig. 5B graphs mean onset latencies (all trials) in each condition. Primary events in all conditions were clear anticipatory inhibitions of dorsal anti-gravity muscles, the BF (thigh extensor/knee flexor) and the ES (back extensor), closely followed by the activation of the TA (ankle flexor). Latencies between anti-gravity muscle inhibitions and TA activation were very small (averages of 30–67 ms, BF; 37–57 ms, ES). Activation of both the RA (trunk flexor) and SCM (neck flexor) anticipated *t0*. Thus, ventral flexor muscles were generally activated in the following bottom-up order: TA-RA-SCM. Following focal movement onset, dorsal anti-gravity extensors, SP

Table 1 Mean displacements of whole- (*CoM*), upper- (*CoMu*), and lower-body (*CoMl*) centers of mass for all subjects and experimental conditions. + Forward displacements, – backward displacements, measured from initial positions. Standard deviations are shown in *parentheses*. Units are shown in m. *D1 N* Distance 1 (5% of height), natural speed; *D1 F* distance 1, fast speed; *D2 N* distance 2 (30% of height), natural speed; *D2 F* distance 2, fast speed
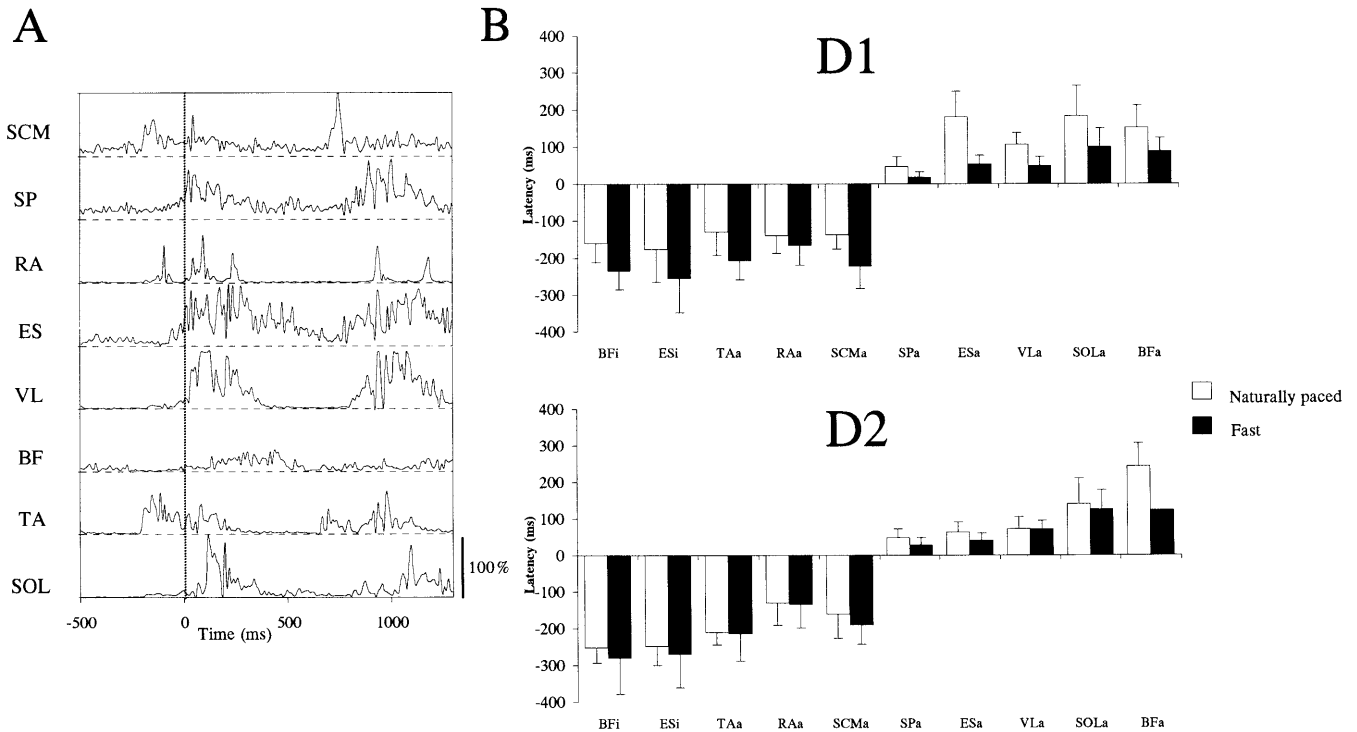
Horizontal displacement (m)					
Center of mass		D1 N	D1 F	D2 N	D2 F
CoM	+	0.050 (0.020)	0.033 (0.021)	0.091 (0.021)	0.067 (0.019)
CoMu	+	0.138 (0.024)	0.11 (0.025)	0.189 (0.026)	0.166 (0.022)
CoMl	–	0.039 (0.018)	0.047 (0.016)	0.019 (0.016)	0.028 (0.022)
	+	0.048 (0.007)	0.005 (0.003)	0.023 (0.011)	0.014 (0.007)

Fig. 5 A Typical EMG activity (D1 F) of the four antagonistic muscle pairs for one subject (S2) between 500 ms before intentional movement onset (*t0*) and the end of reaching. Muscles are: *SOL* soleus, *TA* tibialis anterior, *BF* biceps femoris, *VL* vastus lateralis, *ES* erector spinae, *RA* rectus abdominis, *SP* splenus, *SCM* sterno-cleido mastiodien. **B** Mean inhibition and activation onset latencies (from a total of 72 trials) for all eight muscles in relation to the onset of intentional movement (*t0*) for both distances (*D1*: 5% of height and *D2*: 30% of height) and speeds (naturally paced and fast). *Muscle name + i* Inhibition, *a* activation

(neck extensor), ES (trunk extensor), SOL (ankle plantar flexor), and BF were activated generally in that order. The VL (hip flexor, knee extensor) was activated early following *t0* (on average 48–106 ms), co-contracting with the BF between 87 (D1 F) and 242 ms (D2 N) afterwards. Rare inhibitions of the SOL muscle were recorded only in one subject (S4) in three trials (4%) of two conditions (D1 F and D2 N) from a total of 86 exploited trials. The end of reaching was characterized by the activation of the SOL, TA, VL, ES, and, to some extent, the BF acting to brake the forward displacement of the trunk, and in anticipation of the following lifting phase.

Dynamic effects of anticipatory postural activity

The series of stick figures in Fig. 6A summarizes the evolution of dynamic events associated with whole-body reaching execution at both distances. A similar pattern of events was recorded between N and F conditions, but for clarity only F trials are shown in Fig. 6A. During the period preceding *t0*, F_R was continuously aimed towards the A/P position of the CoM (stick figures 1–4 from the left at each distance in Fig. 6A). Once the CoP began its backward displacement (shown at approximately stick figure no. 5 in Fig. 6A, and in Fig. 6B), F_R (from its origin the CoP) was oriented behind the CoM, creating a negative M_A and, thus, M_X (Fig. 6C). This negative M_X (roughly equivalent to the change in whole-body angular momentum, see Methods) acted counter-clockwise with respect to the CoM in all conditions, provoking the dis-

Table 2 Mean dynamic measures of whole-body reaching initiation (all subjects and experimental conditions). *CoP* Center of pressure backward displacements, M_A moment arm, M_X external moment (negative values = counter-clockwise acceleration of center of mass), F_R resultant ground reaction force (negative values indicate upward directed force or unloading). Units are shown in *parentheses*. Measures were taken in the period between –500 ms before and 500 ms after intentional movement onset (*t0*), and represent maximal values. *D1 N* Distance 1 (5% of height), natural speed; *D1 F* distance 1, fast speed; *D2 N* distance 2 (30% of height), natural speed; *D2 F* distance 2, fast speed
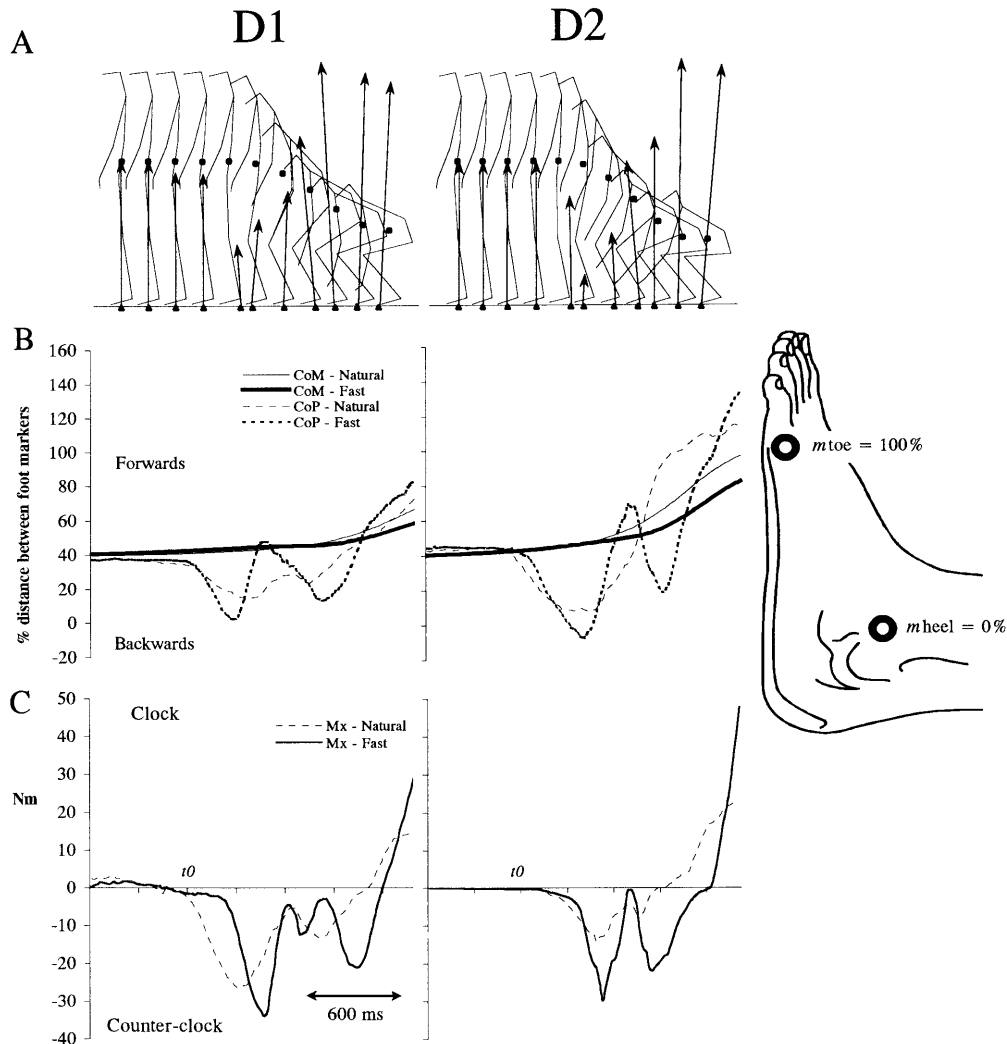
Measure	D1 N	D1 F	D2 N	D2 F
CoP backwards				
% footlength	25.3 (8.1)	40.6 (12.6)	39.8 (9.1)	51.1 (9.5)
MA (m)	–0.042 (0.02)	–0.061 (0.02)	–0.067 (0.02)	–0.086 (0.02)
Mx (Nm)	–26 (7.7)	–35.4 (10.5)	–14.1 (7.1)	–29.8 (14.4)
FR magnitude (N)	182.9 (62.1)	–414.4 (67.3)	–255.6 (79.5)	–482.4 (118.7)

Fig. 6A–C Dynamic events associated with whole-body reaching at both distances D1 (left) and D2 (right). **A**. Vectogram plotting positions of the center-of-mass (*CoM*) (filled circles), CoP (filled triangles), and the magnitude and direction of F_R (resultant ground reaction force) for one typical subject (S6) at both distances (*D1*: 5% of height and *D2*: 30% of height) at fast speed. The magnitude of F_R is scaled as a function of the subjects weight (0.5 cm=100 N). *Arrows* shorter than CoM positions indicate negative (unloaded) F_R values, whilst *longer arrows* represent loading. **B** Typical raw data (all conditions, subject S6), of CoM and center of foot pressure (*CoP*) displacements. The illustration of a foot demonstrates the positions of the external malleolus (*mheel*) and fifth metatarsophalangeal (*mtoe*) markers, and the evolution of the CoM and CoP along the foot length. Displacements of the CoM and CoP were quantified as a percentage of the distance between *m*heel (0%) and *m*toe (100%). **C** The evolution of the external moment (M_X) for all four experimental conditions, corresponding to events shown in **A** and **B**. Indicated are the directions of whole-body angular momentum (clock or counter-clock wise) exerted by the resulting external moment upon the CoM (see **A**). Curves in **B** and **C** are shown from 300 ms before movement onset until the end of reaching and have been normalized temporally to the fastest trial. *t0* Wrist marker movement onset

placement of all body segments (and, thus, the CoM) forwards. Figure 6B shows that, at fast speeds (both distances), a rapid forward inflection of the CoP immediately followed its initial backward displacement. A forward displacement of the CoP with respect to the CoM towards the end of reaching created a positive M_A (and thus M_X), which, coupled with the backward orientation of F_R, accelerated the CoM in a clockwise direction. This may have served to maintain the CoM within the BoS or for the preparation of object lift (Toussaint et al. 1995).

Table 2 lists average measures of the CoP, M_A, M_X, and F_R during the initiation of whole-body reaching. Fig. 6B illustrates, in one typical example, the evolution of the CoP and CoM. Backward displacements of the CoP preceded *t0* by, on average, 124±57 (D1 N), 63±33 (D1 F), 117±52 (D2 N), and 50±47 ms (D2 F). Preceding its backward displacement, the CoP was placed significantly further forwards [$F(1,5)=6.1$, $P<0.01$] along BoS length for movements at D2 than at D1 (average percentages of relative BoS length = 37.3±15.1%, D1 N; 37.5±17.5%, D1 F; 43.2±17.2%, D2 N; and 44.5±11.8%, D2 F). Latencies of CoP backward displacements were significantly correlated with those of TA muscle activation in each condition (D1 N=0.90, D1 F=0.94, D2 N=0.79, and D2 F=0.98). Average displacements of the CoP backwards showed highly significant main effect increases with distance [$F(1,5)=16.8$, $P<0.01$] and speed [$F(1,5)=19.2$, $P<0.001$], with peak backward CoP displacement latencies being correlated to latencies of maximal TA activation (D1 N=0.67, D1 F=0.85, D2 N=0.61, and D2 F=0.80). Increases in CoP backward displacements were accompanied by main effect increases with distance [$F(1,5)=33.8$, $P<0.001$] and speed [$F(1,5)=20.2$, $P<0.001$] in a negative M_A (distance between the CoM and CoP). No interaction effects were seen between distance and speed for both CoP displacements and amplitudes of M_A. Negative values of M_X were greater at D1 than at D2 [$F(1,5)=10.9$, $P<0.01$], regardless of speed (due perhaps to a greater unloading of F_R at D2, Fig. 6A), and showed significant main effect increases with speed [$F(1,5)=20.9$, $P<0.001$].

Discussion

Our findings have shown that, during whole body reaching, opposing displacements of focal and postural segments did not effectively stabilize the CoM, and APAs created the dynamic conditions for forward CoM displacement in different conditions of distance and speed.

Limb-segment kinematics and center-of-mass displacements

The general pattern of segmental displacements (trunk forwards, hip backwards) recorded during whole-body reaching emulated Babinski-type axial strategies previously deemed to minimize displacements of the CoM during forward trunk bending (Crenna et al. 1987). However, despite opposing displacements of the head, shoulder (and knee) with the hip, A/P CoM amplitudes (between 0.032 m, D1 F and 0.091 m, D2 N) exceeded those previously recorded during other forwardly oriented whole-body movements. For example, Crenna et al. (1987) reported CoM amplitudes of 0.010 m (for trunk bending) and, more recently, Commissaris and Toussaint (1997) of 0.025 m during the approach phase of load lifting. Eng et al. (1992) have suggested that, during voluntary movement execution whilst standing, the whole-body CoM can be stabilized by the opposition of upper (focal) and lower (postural) centers of mass. Our results showed an initial opposition of the CoMu with the CoMl (due perhaps to the mechanical effects of forward trunk movements upon lower limbs), after which the CoMl was oriented in a direction similar to both the CoMu and CoM. However, large A/P CoM displacements recorded in our study indicate that the opposition of upper- and lower-body segments was insufficient for stabilizing the CoM in the A/P axis. Supporting lower-body segments played not only a postural, but also a focal role, contributing to whole-body displacements in the direction of the object. Moreover, through recent kinematic simulations (Stapley et al., unpublished observations), we have observed that whole-body reaching movements executed with the CoM constant along the A/P axis (at both distances) represent, in terms of angular configurations, intra-limb, and whole-body dynamics, feasible strategies. We propose, therefore, that the CNS chooses a strategy whereby the CoM is displaced within the BoS, as opposed to ensuring its strict "stabilization".

Axial synergies have been considered to be centrally programmed and devoted to the stabilization of the CoM, which acts as a reference value for posture and movement coordination (Massion 1992). According to this theory, with increases in reaching distance during whole-body reaching, the CNS should have modified segmental strategies to ensure a stabilization of the CoM (for example by displacing the hip further backwards). Indeed, Ramos and Stark (1990) have estimated that, during forward trunk movements, the backward displacement of the hips prevent potential CoM forward displacements of up to 9 cm. Two findings may cast doubt upon the idea of the CoM as the primary stabilized reference during our particular task. First, our results showed that backward hip amplitudes actually reduced with increasing distance (Figs. 1 and 2) and, second, CoM forward displacements attained values (at D2 N) equivalent to those simulated by Ramos and Stark (1990) during trunk movements in the absence of backward hip movements. Nevertheless, some minimization of A/P CoM displacements was evident during fast movements. Our study does not, however, allow us to determine if these reductions were made to fulfill equilibrium or performance constraints of subsequent lifting movements. Indeed, Toussaint et al. (1995) have shown that, to counter perturbing effects of A/P components of F_R during

fast movements, the vertical M_A is increased by increasing the range of CoP displacements and decreasing CoM excursions. This suggests that smaller CoM displacements may be equally related to performance and equilibrium constraints. It must also be considered that, as stability is related to the height of the CoM above the BoS (there is a greater potential to destabilize the body's mass if it concentrated at a position far from the BoS), one strategy that may have been adopted to reduce equilibrium constraints was the lowering of the CoM towards the BoS (indicated by large vertical CoM trajectories).

The relation between electromyographic activity and dynamic postural events

EMG activity associated with the onset of whole-body reaching showed a consistent pattern across experimental conditions (Fig. 5). There was, consistently, a sequential feed-forward inhibition of dorsal antigravity muscles, the BF (thigh extensor / knee flexor) and the ES (back extensor), slightly before the activation of the ankle flexor (TA), trunk prime mover (RA), and neck flexor (SCM). Such a pattern is in accordance with results obtained during forward trunk bending (Crenna et al. 1987), indicating that whole-body reaching can be placed in a similar category of movements. As with trunk bending, two characteristics would suggest that forward segmental (CoM) displacements were centrally programmed. First, the general EMG pattern was highly reproducible across experimental conditions and subjects. Second, TA activation before that of RA would support the idea of a sequential feed-forward activation of postural before prime mover muscles (Belenkii et al. 1967; Crenna et al. 1987) in a distal to proximal fashion (Cordo and Nashner 1982).

The study of APAs during voluntary movements in the standing posture has traditionally been made through the use of EMG activity. In our study, activations of the TA muscle were correlated to displacements of the CoP. As anticipatory inhibition of the SOL muscle was undetected in up to 96% of trials, our results support findings that backward CoP displacements can be obtained by a single component of the motor program associated with the initiation of a range of forwardly oriented movements (Crenna and Frigo 1991). Our results also showed significant increases with distance and speed (corroborating Stapley et al. 1998) in backward CoP displacements and negative values of the M_A. As, in our study, CoM displacements decreased at fast speed, the idea that the primarily controlled variable was the sagittal position of the CoP (under neuromuscular control of the ankle musculature; Okada and Fujiwara 1984) is supported. Examination of dynamic events resulting from APAs would suggest that they did not primarily act to minimize CoM displacements by anticipating forthcoming movement perturbations (Bouisset and Zattara 1981) of arm or trunk movements during whole-body reaching. Following CoP displacement backwards, F_R was orient-

ed behind the CoM, producing forward angular momentum of segments (see Fig. 6A). In light of these and previous results (Stapley et al. 1998), we can confirm that anticipatory postural activity of lower-limb muscles (TA) created necessary forward whole-body angular momentum and CoM displacements, even in smaller-amplitude reaching movements where a stabilization of the CoM could more easily have been assured. It may be argued, however, that backward displacements of the CoP were programmed to accelerate the CoM forwards, counteracting a backward displacement of the CoM induced by forward trunk bending. It is unlikely that all subjects overestimated the intensity of the anticipatory activity required to counter any backward perturbation of the CoM by forward trunk movement, resulting in the marked forward and downward CoM displacements (Fig. 3).

The consistent lack of SOL inhibition and the increase in tonic SOL activity approximately with TA activation onset (see Fig. 5) are interesting observations. During human gait initiation, tonic activity of the stance-limb SOL muscle has been interpreted as increasing ankle stiffness to create a stable postural base during the anticipation phase (Lepers and Brenière 1995). This may have occurred during whole-body reaching initiation, as muscles of the lower leg were responsible not only for the production of a negative external moment (Stapley et al. 1998), but also for equilibrium control. Indeed, an increase in ankle stiffness via antagonist co-activation of SOL and TA would allow equilibrium constraints to dominate over other control mechanisms during this phase. Nevertheless, the absence of SOL inhibition due to cross-talk from the active TA muscle (Solomonow et al. 1994) cannot be ruled out.

Why displace the center of mass?

Our results showed that synergies between upper- and lower-body segments did not ensure a strict stabilization of the CoM, which was displaced forwards by anticipatory lower-limb muscular activity. The question thus arises as to why subjects chose a strategy of CoM displacement within the BoS.

One explanation for displacing the CoM during whole-body reaching may be that stabilizing it at its initial position may have left subjects vulnerable to backward falls due to the incapacity of ankle dorsi-flexors in exerting adequate torque for equilibrium purposes. Indeed, Clément et al. (1988) have shown that highly trained acrobats, when in a handstand position, adopted a forward leaning posture, which was interpreted as a simplifying strategy for the control of destabilizing body oscillations by forearm extensor muscle tone. A similar strategy could be envisaged during whole-body reaching using lower-leg extensor muscles. The standing posture is characterized by a forward body tilt projecting the CoM anterior to the ankle axis of rotation (Gurfinkel 1973). The displacement of the CoM away from the pos-

terior region of the foot during whole-body reaching would have permitted the use of foot length as a dynamic equilibrium area. It may simplify the control of perturbing inertial or gravitational forces acting upon the body from hand trajectory formation and trunk displacement, by SOL or possibly other gastrocnemius activation and resulting ankle plantar flexor torque. One other possibility is that the CoM displacement permits the subject to approach object lift more comfortably, using the extra degree of freedom provided by the forward foot length to generate the necessary backwardly directed angular momentum (Commissaris and Toussaint 1997).

It has also been shown during locomotion that both muscular and gravitational forces are indispensable in the creation of postural and dynamic conditions for CoM forward progression (Prince et al. 1994). During gait initiation, anticipatory TA activation (muscular torque) has been shown to provide initial CoM acceleration, whilst gravitational torque (body weight multiplied by the distance between the CoM and the axis of rotation), produced required CoM velocity at the end of the first step (Lepers and Brenière 1995). Small initial forward trajectories of all three centers of mass in three of the four experimental conditions (see Fig. 3) may have been due to the creation of muscular torques at the ankle by anticipatory TA activation. By displacing the CoM, a similar use of gravitational forces to that described in gait initiation could be envisaged. However, a stabilization of the CoM (at any position within the BoS) would limit the creation of a moment arm between it and the axis of rotation and, thus, the possibility of generating gravitational torque. We propose, therefore, that the anticipatory initiation of whole-body reaching does in fact resemble that of human gait, although executed within a fixed BoS. Indeed, our results showed that the CoP was initially placed further forwards for D2 movements, providing support for such an hypothesis. A greater initial, forward leaning posture preceding the initiation of forward falls permits a more effective use of gravitational force (Dietrich et al. 1994). However, a fundamental question that arises from this study, and which remains to be tested through the direct comparison of whole-body reaching and other forwardly oriented movements (e.g., trunk bending, arm raising), concerns why, in some tasks, there is a stabilization of the CoM, but in others (such as the reaching task studied here) there is not.

Concluding remarks

The present findings show that the coordination between posture and movement during whole-body reaching involves the dynamic (as opposed to static) control of the CoM within the BoS. Our results oppose a great deal of evidence from different voluntary actions, where limb movements are essentially imposed upon static postural configurations (see Massion 1992 for a review). These studies have forwarded the idea that the CoM is the stabilized reference whose displacements are minimized by

axial synergies (Crenna et al. 1987; Alexandrov et al. 1998) or APAs (Bouisset and Zattara 1981, 1987). We suggest, however, that posture and movement coordination must also be associated with CoM displacement within the BoS. A commonly accepted theory is of separate pathways for the control of movement and posture (Massion 1992). Such a theory may not be applicable to whole-body reaching, in view of the fact that postural segments (the hip) participating in the focal aspect of the movement and APAs (centrally programmed in a feedforward manner) created the necessary dynamic conditions for CoM forward displacements. These results corroborate suggestions of a common controller for both focal and postural commands (Aruin and Latash 1995). An alternative possibility is that the division by Hess (1954), Saltzman (1979), and Cordo and Nashner (1982) of postural (*ereismatic*) and focal or instrumental (*teleokinetic*) components of an action may not hold in all conditions of movement. Moreover, it seems that care must be taken when using biomechanical models that attempt to divide segments into these two distinct categories.

Appendix

Validation of the seven-segment model
for CoM calculation

In order to validate the model used to calculate CoM position, differences (in cm) between vertical ground projections of estimated CoM and recorded CoP during quiet stance were determined. Also, the time series of measured and estimated ground reaction forces (Fx and Fz) were compared.

Anthropometric parameters, including segment masses, moments of inertia, and positions of their individual centers of mass, as listed by Plagenhoef et al. (1983), were used to determine CoM positions, as well as net torques and forces generated at each of the joints. The model was considered as an open-loop kinematic chain, applying Langrangian equations of motion to the observed motion of any one joint segment. To determine these values, the seven-segment model was developed as described in the "Materials and methods" section. Assuming that the motion of the body is restricted to the sagittal plane only, the following equations of one-segment motion can be derived:

$$m_i a_{ix} = \sum_j F_{ijx}$$
$$m_i a_{iz} = -m_i g + \sum_j F_{ijz} \tag{1}$$
$$J_i \varepsilon_i = \sum_j (M_{ij} + [\mathbf{R}_{ij} \times \mathbf{F}_{ij}])$$

where *Fijx, Fijy*, and *Mij* are A/P and vertical components of total force, **F**ij, and net torque *M* acted upon joint

Table 3 First column (left hand side): differences (in cm) between vertical ground projections of the center of mass (*CoM*, estimated using the model) and the center of pressure (*CoP*, measured using the platform) during quiet stance (300 ms before movement onset). Positive and negative values indicate that the CoM was in front of and behind the CoP, respectively. Second and third columns: average correlation coefficients calculated between time series of *Fx* and *Fz* components of the ground reaction force derived from the seven-segment model and those measured directly from the force platform for the six subjects (four trials) and each experimental condition for the whole of the reaching movements. *D1 N* Distance 1 (5% of height), natural speed; *D1 F* distance 1, fast speed; *D2 N* distance 2 (30% of height), natural speed; *D2 F* distance 2, fast speed

Subject	D1 N			D1 F			D2 N			D2 F		
	CoM-CoP (cm)	*Fx*	*Fz*	CoM-CoP (cm)	*Fx*	*Fz*	CoM-CoP (cm)	*Fx*	*Fz*	CoM-CoP (cm)	*Fx*	*Fz*
1	−1.48	0.54	0.98	−1.47	0.53	0.98	−1.42	0.66	0.98	−1.41	0.61	0.98
2	0.8	0.79	0.98	0.47	0.72	0.98	1.15	0.79	0.99	0.24	0.77	0.98
3	1.24	0.78	0.97	0.75	0.81	0.98	2.32	0.93	0.98	1.52	0.86	0.98
4	−0.46	0.75	0.97	−0.46	0.68	0.98	−0.11	0.9	0.98	2.35	0.84	0.97
5	0.04	0.71	0.96	−0.38	0.69	0.96	0.48	0.7	0.98	0.37	0.65	0.97
6	0.03	0.73	0.98	−0.16	0.8	0.98	0.57	0.86	0.98	0.13	0.86	0.98
Mean	0.03	0.72	0.97	−0.21	0.71	0.98	0.48	0.81	0.98	0.53	0.77	0.98
SD	0.96	0.09	0.01	0.78	0.1	0.01	1.23	0.11	0	1.29	0.11	0.01

j of the segment *i*, respectively. **R***ij* is a radius vector drawn from the *i*th segment's CoM to the joint center *j*. *mi*, *Ji*, *aix*, *aiz,εi* represent, respectively, a segments mass, its moment of gyration relative to the CoM, A/P and vertical components of the vector of CoM acceleration, and angular acceleration of the segment around an axis perpendicular to the plane of motion. *g* is the free-fall acceleration due to gravity. The acceleration of a segments' CoM, *ai*, and its angular acceleration were calculated using observed A/P and vertical co-ordinates, its length, *l*, and accelerations of proximal and distal ends.

To derive whole-body components of *Fx*, *Fy*, *Fz*, and the CoP, the motion of a system can be regarded as the motion of its CoM and the motion around its CoM. This means that two vector equations can be established: (1) the vector sum of all the external forces equal to the system's mass multiplied by the vector of CoM acceleration, and (2) the vector sum of all torques relative to the CoM, called the tensor of inertia relative to the CoM. For 2D motion, these two vector equations provide three scalar equations:

$$Fx = m \cdot \mathbf{a}x \quad Fz = m \cdot \mathbf{a}z \quad Mz = j \cdot \dot{w}$$

where *Fx* and *Fz* are components of the total force acted upon the system (including gravitational force), *Mz* is the total torque relative to the system's CoM, *ax* and *az* are components of CoM acceleration, ·*w* is the system's angular acceleration, *m* is the system's mass, and *j* is the moment of gyration relative to the CoM. When considering one segment at a time, these three equations give three values for *Fx*, *Fz*, and *Mz*, acted at each of an *n* number of joints. Using the open-loop kinematic chain, it was possible to calculate, step-by-step from the most distal segment, these three values to the ground segment. Thus, ground reaction forces (*Fx* and *Fz*) are taken as those calculated in the final joint of the chain (the ankle).

To compare functions estimated using the model and those taken directly from the platform Pearson product, moment correlation coefficients between the sum of squares for each component (for example, *Fx*) were calculated using the following formula:

$$r = \sum \frac{\sqrt{Fx\_Cl} - Fx\_Pl}{\sum \sqrt{Fx\_Pl}}$$

where *Fx_Cl* is the A/P ground reaction force calculated using the kinematic model, and *Fx_Pl* is that derived directly from the platform.

Differences (in cm) between mean vertical projections of estimated CoM and recorded CoP positions are shown for all subjects and experimental conditions in Table 3 (left column of each condition). Mean differences between the two ranged from 0.03 cm (D1 N) to 0.53 cm (D2 F). These values were slightly higher than those reported by Kingma et al. (1995), who validated a nine-segment model for lifting. This may have been due to errors that exist in documented mass, CoM, and inertial parameters of each segment involved in whole-body CoM calculation.

In the second and third columns of each condition in Table 3, statistically significant correlation coefficients calculated between estimated and recorded *Fx* and *Fz* times series are shown. Mean correlation coefficients ranged between *r*=0.71 (*Fx*, D1 F) and *r*=0.98 (*Fz*, D1 F, D2 N, and D2 F). It must be noted that coefficients were consistently lower for *Fx* than for *Fz*. As *Fx* values are habitually smaller than those of Fz, this may have been due to the signal-to-noise ratio being lower in the A/P than in the vertical direction (assuming that the noise level is equal along both axes). However, significant correlation coefficients obtained for the comparison between estimated and recorded ground reaction forces in the present study are comparable, if not higher than those reported by Looze et al. (1992), and more recently Kingma et al. (1996).

It may be concluded, therefore, that the model used in the present study provided realistic trajectories of whole, postural, and focal centers of mass.

References

Alexandrov A, Frolov A, Massion J (1998) Axial synergies during human upper trunk bending. Exp Brain Res 118:210–220

Aruin AS, Latash ML (1995) The role of motor action in anticipatory postural adjustments studied with self-induced and externally triggered perturbations. Exp Brain Res 106:291–300

Babinski J (1899) De l'asymmetrie cérébelleuse. Rev Neurol (Paris) 7:806–816

Basmajian JV (1978) Muscles alive: their functions revealed by electromyography. Williams and Wilkins, Baltimore USA

Belenkii YY, Gurfinkel V, Paltsev Y (1967) Elements of control of voluntary movements. Biofizika 12:135–141

Bouisset S, Zattara M (1981) A sequence of postural movements precedes voluntary movement. Neurosci Lett 22:263–270

Bouisset S, Zattara M (1987) Biomechanical study of the programming of anticipatory postural adjustments associated with voluntary movement. J Biomech 20:735–742

Brenière Y, Do MC, Bouisset S (1987) Are dynamic phenomena prior to stepping essential to walking? J Mot Behav 19:62–76

Clément G, Pozzo T, Berthoz A (1988) Contribution of eye positioning to control of the upside-down standing posture. Exp Brain Res 73:569–576

Commissaris DACM, Toussaint H (1997) Anticipatory postural adjustments in a bimanual, whole body lifting task with an object of unknown weight. Hum Mov Sci 16, 407–431

Cordo PJ, Nashner LM (1982) Properties of postural adjustments associated with rapid arm movements. J Neurophysiol 47:287–302

Crenna P, Frigo C (1991) A motor programme for the initiation of forward oriented movements in humans. J Physiol 437:635–653

Crenna P, Frigo C, Massion J, Pedotti A (1987) Forward and backward axial synergies in man. Exp Brain Res 65:538–548

Dietrich G, Brenière Y, Do MC (1994) Organisation of local anticipatory movements in single step initiation. Hum Mov Sci 13:195–210

Droulez J, Berthoz A (1986) Servo-controlled (conservative) versus topological (projective) modes of sensory motor control. In: Bles W, Brandt T (eds) Disorders of posture and gait. Elsevier, Amsterdam, pp 83–97

Eng JJ, Winter DA, MacKinnon CD, Patla AE (1992) Interaction of the reactive moments and center of mass displacement for postural control during voluntary arm movements. Neurosci Res Commun 11:73–80

Gurfinkel VS (1973) Physical foundations of the stabilography. Agressologie 14:9–14

Hess WR (1954) Telekinetisches und ereismatisches Kräftesystem in der Biomotorik. Helv Physiol Pharmacol Acta 1:C62-C63

Kingma I, Toussaint HM, Commissaris DACM, Hoozemans MJM, Ober MJ (1995) Optimizing the determination of the body center of mass. J Biomech 28:1137–1142

Kingma I, Looze MP de, Toussaint HM, Klijnsma JG, Bruijnen TBM (1996) Validation of a full body 3-D dynamic linked segment model. Hum Mov Sci 15:833–860

Lee WA, Micheals CF, Pai YC (1990) The organisation of torque and EMG activity during bilateral handle pulls by standing humans. Exp Brain Res 82:304–314

Lepers R, Brenière Y (1995) The role of anticipatory postural adjustments and gravity in gait initiation. Exp Brain Res 107:118–124

Looze MP de, Kingma I, Bussmann JBJ, Toussaint HM (1992) Validation of a dynamic linked segment model to calculate joint moments in lifting. Clin Biomech 7:161–169

Marsden CD, Merton PA, Morton HP (1981) Human postural responses. Brain 104:513–534

Massion J (1992) Movement, posture and equilibrium: interaction and coordination. Prog Neurobiol 38:35–56

Massion J, Popov K, Fabre JC, Rage P, Gurfinkel VS (1997) Is the erect posture in microgravity based on the control of trunk orientation or center of mass position? Exp Brain Res 114:384–389

Mergner T, Siebold C, Schweigart G, Becker W (1991) Human perception of horizontal trunk and head rotation in space during vestibular and neck stimulation. Exp Brain Res 85:389–401

Mouchnino L, Aurenty R, Massion J, Pedotti A (1992) Coordination between equilibrium and head-trunk orientation during leg movement: a new strategy built up by training. J Neurophysiol 67:1587–1598

Mouchnino L, Aurenty R, Massion J, Pedotti A (1993) Is the trunk a reference frame for calculating leg position? Neuroreport 4:125–127

Mouchnino L, Cincera M, Fabre JC, Assaiante C, Amblard B, Pedotti A, Massion J (1996) Is the regulation of the center of mass maintained during leg movement under microgravity conditions? J Neurophysiol 76:1212–1223

Nardone A, Schieppati M (1988) Postural adjustments associated with voluntary contraction of leg muscles in standing man. Exp Brain Res 69:469–480

Oddsson L (1988) Coordination of a simple voluntary multi-joint movement with postural demands: trunk extension in standing man. Acta Physiol Scand 134:109–118

Okada M, Fujiwara K (1984) Relation between sagittal distribution of the foot pressure in upright stance and relative EMG magnitude in some leg and foot muscles. J Hum Ergol (Tokyo) 13:97–105

Pedotti A, Crenna P, Deat A, Frigo C, Massion J (1989) Postural synergies in axial movements: short and long term adaptation. Exp Brain Res 74:3–10

Plagenhoef S, Gaynor Evans FG, Abdelnour T (1983) Anatomical data for analyzing human motion. Res Q Exerc Sport 54:169–178

Pozzo T, Berthoz A, Lefort L (1990) Head stabilization during various locomotor tasks in humans. I. Normal subjects. Exp Brain Res 82:97–106

Pozzo T, Levik Y, Berthoz A (1995) Head and trunk movements in the frontal plane during complex equilibrium tasks in humans. Exp Brain Res 106:327–338

Pozzo T, McIntyre J, Cheron G, Papaxanthis C (1998) Hand trajectory formation during whole body reaching movements in man. Neurosci Lett 240:159–162

Prince F, Winter DA, Stergiou P, Walt SE (1994) Anticipatory control of upper body balance during human locomotion. Gait Posture 2:19–25

Ramos CF, Stark LW (1990a) Postural maintenance during movement: simulations of a two joint model. Biol Cybern 63:363–375

Ramos CF, Stark LW (1990b) Postural maintenance during fast forward bending: a model simulation experiment determines the 'reduced trajectory'. Exp Brain Res 82:651–657

Saltzman E (1979) Levels of sensorimotor representation. J Math Psychol 20:91–163

Sergio LE, Ostry DJ (1994) Coordination of mono- and bi-articular muscles in multi-degree of freedom elbow movements. Exp Brain Res 97:551–555

Solomonow M, Baratta R, Bernadi M, Zhou B, Lu Y, Acierno S (1994) Surface and wire EMG cross-talk in neighbouring muscles. J Electromyogr Kinesiol 4:131–142

Stapley P, Pozzo T, Grishin A (1998) The role of anticipatory postural adjustments during forward whole body reaching. Neuroreport 9:395–401

Toussaint HM, Commissaris DACM, Dieën JH van, Reijnen JS, Praet SFE, Beek PJ (1995) Controlling the ground reaction force during lifting. J Mot Behav 27:225–234